Deadbeat Weighted Average Current Control With Corrective Feed-Forward Compensation for Microgrid Converters With Nonstandard *LCL* Filter

Jinwei He, *Member, IEEE*, Yun Wei Li, *Senior Member, IEEE*, Dehong Xu, *Fellow, IEEE*, Xiaodong Liang, *Senior Member, IEEE*, Beihua Liang, and Chengshan Wang, *Senior Member, IEEE*

***Abstract*—Microgrid converters are required to have the capability of both grid-tied mode and islanding mode operation. For this dual-mode operation, large shunt capacitors are often used in the interfacing converter output *LCL* filter, as it can help to stabilize supply voltage and to reduce switching ripple pollutions to sensitive loads during autonomous islanding operation. At the same time, this modification causes a few challenges, including the low-frequency harmonic distortions, the steady-state tracking errors and the slow dynamic response, to the line current regulation during grid-tied operation. To overcome these drawbacks, a modified weighted average current controller is developed. First, to realize a fast line current response, a deadbeat control of weighted average current is developed based on a reduced-order virtual filter plant. Second, a grid voltage feed-forward term is added to the weighted average current reference to mitigate the steady-state line current tracking errors. Note that this compensation term is directly added to the current reference, thus, it is very well decoupled from the closed-loop current regulator. In addition, it can be seen that the low-order line current harmonics caused by grid voltage distortion is inherently compensated by this proposed corrective feed-forward control.**

***Index Terms*—Active damping, deadbeat control, *LCL* filter, microgrid, virtual filter, weighted average current control.**

I. Introduction

With the growing penetration of distributed generation (DG) units in low- and medium-voltage power distribution systems, microgrid has been popularized in order to realize better operation of multiple DG systems [1]–[3]. Compared to a conventional grid-tied converter with only grid-tied operation capability, the microgrid application usually requires an interfacing converter to provide continued electricity to local critical loads in the case of utility grid interruptions [3]–[5], [26]. Thus, a microgrid interfacing converter is often named as "dual-mode" converter. Conventionally, an interfacing converter with only a single series choke can be used for both grid-tied and islanding operation. However, the series choke is bulky and the switching ripples can be injected into the grid or the local sensitive loads [17]. Thus, the selection of series choke-based filter is mainly determined by the grid integration requirement and the type of local load. As a better solution, the smaller size *LCL* filter is also widely adopted and the capacitor voltage of the *LCL* filter shall be controlled in islanding operation mode [7], [8]. Note that for an islanding operation, a relatively large filter capacitor is often needed to minimize the supply voltage ripples [9]–[11]. However, this modification of filter capacitor may violate a few *LCL* filter design criteria that mainly focus on the operation of converters in grid-connected mode [12]–[14], [44]. Due to the adoption of large shunt capacitors, the cutoff frequency of *LCL* filter may be too low to ensure good control of the line current. Specifically, the following problems often appear:

1) line current can be more distorted with low-frequency resonances, due to the decrease of *LCL* filter resonance frequency;
2) there are noticeable steady-state tracking errors in the line current, as the filter plant response has lower open-loop gain and larger phase shift at around the fundamental frequency. In addition, the dynamic response of the line current can be affected.

To address the first problem, active damping is considered as an effective tool [15], [35]–[39], [45]. Among all these methods, the internal mode line current control methods with active damping, such as the single-loop control with lead–leg compensators [14], [39] and the double-loop cascaded current regulator [16] , [36]–[38], maybe the most well understood options. In addition, a few active damping methods, such as using the nonlinear control in [18], the adaptive control in [20], and the observer-based control in [20] have been reported in the recent literature. When using these advanced current controllers, the computational load for interfacing converter microcontroller may increase and the parameter tuning is not very straightforward. Alternatively, the control of weighted average of inverter output current and line current is also proposed [21]–[23]. It can be seen that the resonance of the filter is easily mitigated by using weighted average current controller, but the line current is not directly regulated. It is also necessary to note that when relatively large shunt capacitor is used in the output filter and the grid voltage or

Manuscript received September 4, 2015; revised November 21, 2015, February 8, 2016, and April 18, 2016; accepted May 20, 2016. Date of publication June 13, 2016; date of current version January 20, 2017. Recommended for publication by Associate Editor S. Golestan.

J. He, B. Liang, and C. Wang are with theKey Laboratory of Smart Grid of Ministry of Education, Tianjin University, Tianjin 300072, China (e-mail: hjinwei@ualberta.ca; bhliang@tju.edu.cn; cswang@tju.edu.cn).

Y. W. Li is with the Department of Electrical and Computer Engineering, University of Alberta, Edmonton, AB T6G 2V4 Canada (e-mail: yunwei.li@ualberta.ca).

D. Xu is with the Institute of Power Electronics, College of Electrical Engineering, Zhejiang University, Hangzhou 310027, China (e-mail: xdh@cee.zju.edu.cn).

X. Liang is with the Faculty of Engineering and Applied Science, Memorial University of Newfoundland, St. John's, NL A1B 3X9 Canada (e-mail: xliang@mun.ca).

Color versions of one or more of the figures in this paper are available online at http://ieeexplore.ieee.org.

Digital Object Identifier 10.1109/TPEL.2016.2580005

the local load has significantly harmonic distortions, the shunt capacitor branch essentially provides a low-impedance branch to pass through harmonic current excited by grid harmonic voltage or local load [41]. In this case, the effectiveness of many conventional active damping methods has not been examined.

When the grid voltage is highly distorted, its impact on the line current tracking must be properly addressed [55]. A good option to solve this problem is to use point of common coupling (PCC) voltage-based feed-forward terms. In [38], [52], and [53], the full-feed-forward control term is added to a double-loop controller to reject the impact of grid voltage distortions in a wide-frequency range. In addition, an interesting bandpass filter-based feed-forward control method was recently proposed in [54] to reject the impact of grid voltage harmonics at a few selected harmonic frequencies. Through the detailed analysis in [54], it can be known that the abovementioned methods essentially reduce the admittance of the converter closed-loop equivalent circuit to enhance line current quality. Nevertheless, these compensation terms are highly relevant to the parameters of the current regulator and they are usually added to the inner loop current reference or voltage reference of the system. Therefore, current regulators and compensation terms should be designed together to get an improved performance. It would be favorable if the compensation term and current regulators can be decoupled to simplify the parameter design procedure.

To address the second problem as indicated above, the rapid current controller can be used [24]. It has been evaluated in [15], [27], [46], [49] that various types of current controller, including proportional and integral (PI) controller, proportional and resonant (PR) controller, and deadbeat controller, can realize similar fast dynamic response. However, only the inverter output current is controlled in [15]. In this case, the offset current from the filter capacitor leg is not compensated. As an accurate power control is needed for DG interfacing converter, the closed-loop power regulation scheme, such as that in [48], can be adopted. Nevertheless, this control could further increase the computational load of DG controllers. To remove the closed-loop power regulators, the open-loop power control through direct regulation of line current reference is also widely accepted. In this case, the accurate control of line current is needed but the impact of large shunt filter capacitor could affect both the dynamic response and the steady-state tracking accuracy of line current [41]. To the best of our knowledge, this specific problem has rarely been researched in the previous literature. Therefore, a schematic study of current controllers for microgrid converters with nonstandard output filter is definitely necessary.

In this paper, a quasi-deadbeat controller is developed to maintain both rapid line current response and proper resonance damping, even for a dual-mode converter with nonstandard *LCL* filter. First, a reduced-order virtual filter plant is established and the deadbeat control of weighted average current is designed without the involvement of shunt capacitor of the *LCL* filter. In addition, to reduce the existing steady-state line current errors caused by using the weighted average current approximation and the harmonics caused by grid voltage disturbances, a corrective grid voltage feed-forward term is developed for the proposed deadbeat controller. With the aforementioned two steps, an accurate and a fast line current control can be achieved even for dual-mode microgrid converter with adverse *LCL* filter parameters.

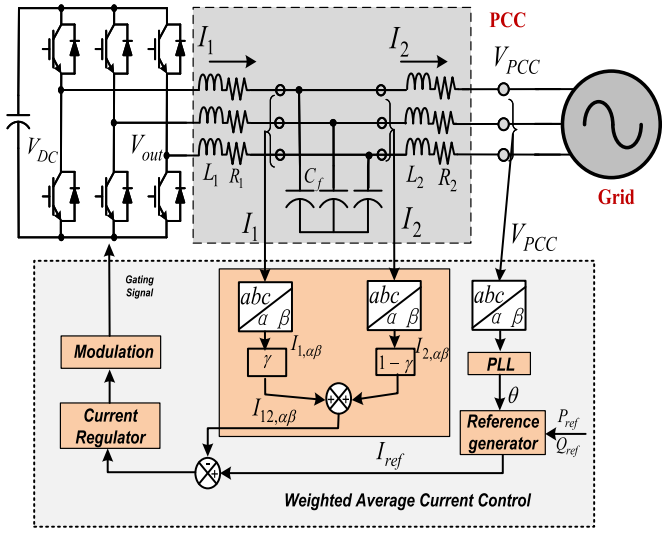

Fig. 1. Diagram of a grid-tied converter controlled by conventional weighted average current feedback.

II. Weighted Average Current Control

The control of grid-tied converter using the conventional weighted average current feedback is briefly reviewed in this section, with emphasis on the filter resonance and the line current control accuracy.

A. Principle of Weighted Average Current Control

The upper part of Fig. 1 shows a diagram of a three-phase grid-tied system. The inverter bridge is connected to the PCC via an *LCL* filter. The inverter side choke inductance is L_1 and the stray resistance is R_1. The grid-side choke inductance is L_2 and the stray resistance is R_2. The capacitance of shunt capacitor and the equivalent series resistor (ESR) or passive damping resistor in the middle of the filter are C_f and R_f, respectively.

There are two types of ac current measurements, inverter output current $I_{1,\alpha\beta} = [I_{1,\alpha}, I_{1,\beta}]^T$ and line current $I_{2,\alpha\beta} = [I_{2,\alpha}, I_{2,\beta}]^T$ in this system. Note that the subscript $\alpha\beta$ in this paper is also applicable to a vector with two components in the α and β reference frame. For an internal mode current regulator, such as a conventional single-loop PI control or PR control, either the inverter output current $I_{1,\alpha\beta}$ or the line current $I_{2,\alpha\beta}$ can be chosen as the feedback. Note that single-loop control schemes often suffer from *LCL* filter resonances, and accordingly, a stringent constraint of the controller open-loop gain is required to ensure the stability of the system. Due to this limitation, the line current tracking dynamics using a conventional single-loop PI or PR control is typically slow, particularly when the output filter has a relatively low cutoff frequency due to the adoption of large shunt capacitors.

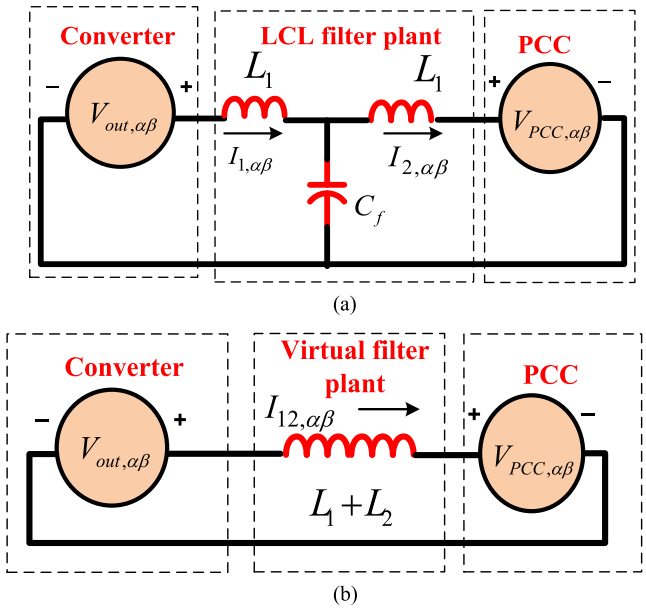

Fig. 2. Diagram of a grid-tied converter controlled by conventional weighted average current feedback. (a) Per-phase equivalent circuit of the *LCL* filter. (b) Per-phase equivalent circuit of the virtual filter.

To avoid this limitation, an interesting weighted average current feedback as shown in the lower part of Fig. 1 was recently proposed [22] [23]. The weighted average current $I_{12,\alpha\beta}$ in the two-axis stationary reference frame is expressed as

$$I_{12,\alpha\beta} = \gamma \cdot I_{1,\alpha\beta} + (1-\gamma) \cdot I_{2,\alpha\beta} \tag{1}$$

where the weighting factor Υ is determined according to the inductance ratio of two series chokes in the *LCL* filter as follows:

$$\gamma = \frac{L_1}{L_1 + L_2}. \tag{2}$$

Since the output *LCL* filter circuits in the $\alpha - \beta$ reference frame are decoupled, a per-phase output *LCL* filter circuit as shown in Fig. 2(a) is used for illustration. The response of the output current $I_{1,\alpha\beta}$ and the line current $I_{2,\alpha\beta}$ can be easily obtained as follows:

$$I_{1,\alpha\beta} = G_{11}(s) \cdot V_{\text{out},\alpha\beta} - G_{12}(s) \cdot V_{\text{PCC},\alpha\beta} \tag{3}$$

$$I_{2,\alpha\beta} = G_{21}(s) \cdot V_{\text{out},\alpha\beta} - G_{22}(s) \cdot V_{\text{PCC},\alpha\beta} \tag{4}$$

where $V_{\text{out},\alpha\beta}$ and $V_{\text{PCC},\alpha\beta}$ are the inverter output voltage and PCC voltage, respectively. The gains $G_{11}(\text{s})$ to $G_{22}(\text{s})$ in (3) and (4) can be derived based on a per-phase circuit as follows:

$$G_{11}(s) = \frac{z_2 + z_c}{z_1 z_2 + z_1 z_c + z_2 z_c},\ G_{12}(s) = \frac{-z_c}{z_1 z_2 + z_1 z_c + z_2 z_c}$$

$$G_{21}(s) = \frac{z_c}{z_1 z_2 + z_1 z_c + z_2 z_c},\ G_{22}(s) = \frac{-(z_1 + z_c)}{z_1 z_2 + z_1 z_c + z_2 z_c}$$

where $z_1 = sL_1 + R_1,\ z_2 = sL_2 + R_2$, and $z_C = 1/sC_f$.

By substituting (3) and (4) for the line current $I_{2,\alpha\beta}$ and the output current $I_{1,\alpha\beta}$ in (1), the weighted average current can be expressed as follows:

$$\begin{aligned} I_{12,\alpha\beta} = {} & \gamma \cdot (G_{11}(s) \cdot V_{\text{out},\alpha\beta} - G_{12}(s) \cdot V_{\text{PCC},\alpha\beta}) \\ & + (1-\gamma) \cdot (G_{21}(s) \cdot V_{\text{out},\alpha\beta} - G_{22}(s) \cdot V_{\text{PCC},\alpha\beta}). \end{aligned} \tag{5}$$

Reorganizing (5) and ignoring the small stray resistance R_1 and R_2 of the series chokes, the response of the weighted average current to inverter output voltage and PCC voltage can be simply obtained as follows:

$$\begin{aligned} I_{12,\alpha\beta} &= \frac{V_{\text{out},\alpha\beta} - V_{\text{PCC},\alpha\beta}}{(L_1 + L_2) \cdot s} \\ &= G_{I12-\text{Vout}}(s) \cdot (V_{\text{out},\alpha\beta} - V_{\text{PCC},\alpha\beta}). \end{aligned} \tag{6}$$

When the weighted average current $I_{12,\alpha\beta}$ is selected as a control objective, a third-order *LCL* filter plant with a resonant peak can be transformed into a first-order virtual filter that only consists of two series inductors, as shown in Fig. 2(b). The transfer function is depicted as $G_{I12-\text{Vout}}(s) = 1/(L_1 + L_1)s$. In this case, the response of the weighted average current $I_{12,\alpha\beta}$ can be regulated by controlling the voltage difference across the series virtual choke $L_1 + L_2$. With this virtual filter plant, the resonance of an *LCL* filter can be mitigated without any additional active control.

In the previous research, both the PR controller in the stationary reference frame [22] and the PI controller in the synchronous rotating reference frame [23] have been applied to control the weighted average current. Due to the favorable feature of weighted average current measurement, PR and PI with higher loop gains can be used to realize a faster tracking of weighted average current $I_{12,\alpha\beta}$. It has been reported in [8] that the WAC is equivalent to add a virtual damping impedance in parallel with the *LCL* filter capacitor leg. Thus, the resonance peak can be effectively attenuated. On the other hand, Shen *et al.* [22] also pointed out that the stability of the system can still be sensitive to very high-current regulator loop gains. To overcome this limitation, a small passive damping resistor in series with shunt filter capacitor is needed in some circumstances and the PI/PR control parameters should be properly designed.

B. Frequency Domain Analysis

As the weighted average current feedback provides an effective way to simplify the current controller design and to mitigate the resonance of grid-tied converters, it was intensively studied in recent research work. This section further conducts an analysis of the weighted average current feedback algorithm with emphasis on the line current tracking accuracy and the resonance damping in adverse situations.

1) Current Tracking Accuracy: Considering that the line current is directly injected into the utility grid but only the weighted average current is involved in the closed-loop current control, the difference between the weighted average current and the line current is calculated here. First, it is easy to get:

$$I_{1,\alpha\beta} = I_{2,\alpha\beta} + I_{c,\alpha\beta} \tag{7}$$

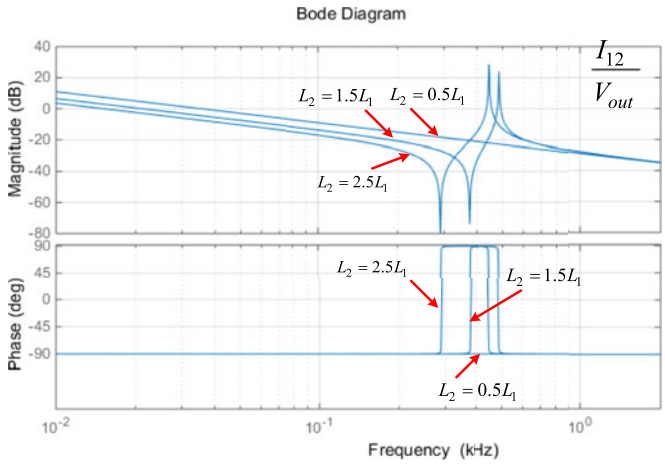

Fig. 3. Open-loop response of weighted average current considering filter parameter variation.

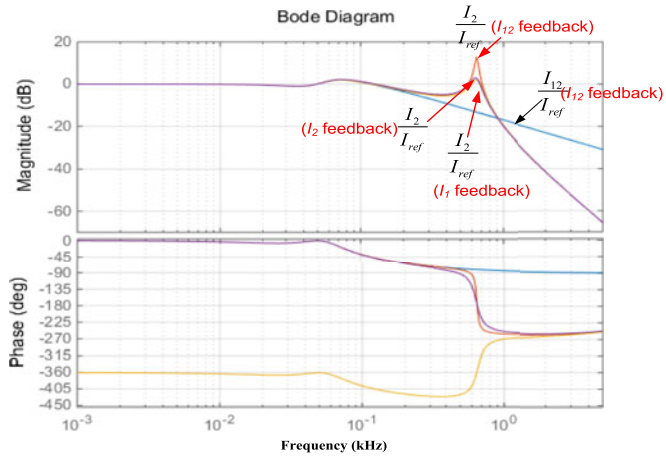

Fig. 4. Closed-loop response of line current I_2 and weighted average current I_{12} when various types of current measurements are adopted.

where $I_{c,\alpha\beta}$ is the *LCL* filter capacitor current. Then, the difference between $I_{12,\alpha\beta}$ and $I_{2,\alpha\beta}$ is given as follows:

$$\begin{aligned} I_{12,\alpha\beta} - I_{2,\alpha\beta} &= [\gamma \cdot I_{1,\alpha\beta} + (1-\gamma) \cdot I_{2,\alpha\beta}] - I_{2,\alpha\beta} \\ &= [\gamma \cdot (I_{2,\alpha\beta} + I_{c,\alpha\beta}) \\ &\quad + (1-\gamma) \cdot I_{2,\alpha\beta}] - I_{2,\alpha\beta} \\ &= \gamma \cdot I_{c,\alpha\beta}. \end{aligned} \tag{8}$$

When the filter converter side choke inductance L_1 is much higher than the grid-side inductance L_2, such as the case of using only isolation transformer leakage inductance as L_2, the weighting factor can be close to 1. Accordingly, the weighted average current I_{12} is close to I_1. In this case, the current flowing through the filter capacitor can cause noticeable line current control errors.

As mentioned earlier, dual-mode operation of a converter needs relatively large shunt capacitors in the *LCL* filter to minimize supply voltage ripples in the standalone islanding operation. From (8), it can be seen that the adopted large capacitor could further aggravate the line current tracking errors when the weighted average current is selected as the control objective.

2) Filter Resonance: The changes of *LCL* filter parameters, especially the uncertainty of line side inductance L_2, may also affect the performance of a system using the weighted average current feedback. When filter parameters have noticeable variations, the weighted average current I_{12} to inverter output voltage V_{out} cannot be ideally simplified as a first-order system and the open-loop response may have a resonant peak. Fig. 3 shows the performance of the system with varying line side inductance L_2, but a fixed weighting factor Υ is determined according to an assumption that $L_2 = 0.5L_1$. The parameters of the filters are listed as $L_1 = 3\,\text{mH}$, $L_2 = 1.5\,\text{mH}$, and $C_f = 60\,\mu\text{F}$. It can be seen that when the inductance L_2 is a half of L_1, the weighted average current I_{12} has a linear response to converter output voltage V_{out}. On the other hand, the response has a resonant peak at around 571 Hz when L_2 is 1.5 times larger than L_1. This resonance moves to 498 Hz and its magnitude is further amplified when a larger $L_2 = 3.75\,\text{mH}$ is adopted.

Since the line current I_2 is selected as the final control objective, the closed-loop responses of line current and the weighted average current are also compared in Fig. 4. First, the response of line current is studied when different measurements (I_1 and I_2) are used in the single closed-loop current control. The PR controller as shown in [14] is used as the current regulator. In this case, the proportional and resonant gains are 4 and 255, respectively. It can be easily seen that the conventional PR control using only single current feedback cannot mitigate the response peak at around 500 Hz.

On the other hand, when the weighted average current is selected as the feedback, the closed-loop responses of weighted average current and line current are provided in Fig. 4. It shows that the response of weighted average current I_{12} has very low gain at high-frequency region to suppress the harmonics in I_{12} However, even in the case of using weighted average current as the feedback, the response of line current I_2 has a high closed-loop gain at around 650 Hz. This is mainly because the offset of capacitor current is not fully compensated by the weighted average current control [22]. As a result, weighted average current control might adversely cause some resonances when a large shunt capacitor is selected for the *LCL* filter.

III. Proposed Deadbeat Control

Since the conventional weighted average current control may cause resonance problem in dual-mode converter grid-tied operation and the line current tracking has some steady-state errors, a deadbeat current controller with feed-forward term is proposed to overcome these problems. This section is organized as follows. First, the capacitor current is estimated in the continuous s-domain and then its discretized expression in the z-domain is given. Second, the discrete-time domain expression of deadbeat controller for weighted average current control is obtained based on the virtual filter plant. Finally, the characteristics of a

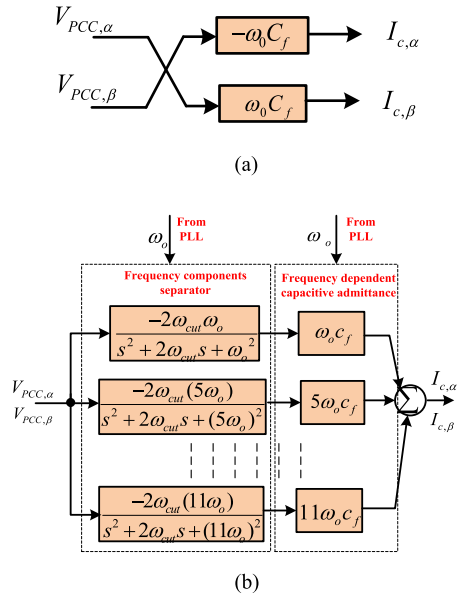

Fig. 5. Diagram of the capacitor current estimator. (a) Capacitor current estimation using voltage cross-coupling feed-forward. (b) Frequency Selective capacitor current estimation.

converter using the proposed method are analyzed by using root loci and Bode plots.

A. Current Tracking Error Estimation

To improve the line current tracking accuracy, the offset term (8) as shown in the previous section shall be properly compensated. Considering the capacitor current measurement is typically not available in a grid-tied converter system and the PCC voltage is measured for grid synchronization, an estimator using the detected PCC voltage as the input is proposed here as Fig. 5. First, considering the voltage drop on the line side inductor I_2 is small comparing to the magnitude of PCC voltage, the capacitor current can be approximated as follows:

$$I_{\mathrm{cap},\alpha\beta} = sC_f \cdot V_{C,\alpha\beta} \approx sC_f \cdot V_{\mathrm{PCC},\alpha\beta} \tag{9}$$

where s is a differential operator.

As the differential operation of PCC voltage may amplify the high-frequency noise at PCC, a practical estimation method is discussed here. When the PCC voltage has small disturbance due to the strict requirement of the PCC voltage quality and considering that the fundamental frequency component of filter capacitor current is the root cause for the line current tracking error, the capacitor current can be estimated through a simple cross-coupled voltage feed-forward term as follows:

$$I_{\mathrm{cap},\alpha\beta} \approx sC_f \cdot V_{\mathrm{PCC},\alpha\beta} \approx j\beta\omega_0 C_f \cdot V_{\mathrm{PCC},\alpha\beta} \tag{10}$$

where ω_0 is the fundamental angular frequency determined by the phase-locked loop (PLL). When (10) is expressed in the real and imaginary axis, it is easy to get

$$\begin{aligned} I_{\mathrm{cap},\alpha\beta} &= I_{c,\alpha} + jI_{c,\beta} = j\omega_f c_f V_c \approx j\omega_f c_f V_{\mathrm{PCC}} \\ &= j\omega_f c_f (V_{\mathrm{PCC},\alpha} + jV_{\mathrm{PCC},\beta}) \\ &= -\omega_f c_f V_{\mathrm{PCC},\beta} + j\omega_f c_f V_{\mathrm{PCC},\alpha} \end{aligned} \tag{11}$$

On the other hand, according to the emerging fault ride-through concept, an interfacing converter is also required to have continued operation even when the main grid voltage has significant distortions. In this case, the impact of the grid voltage harmonics must be properly considered when estimating the capacitor current. A frequency-selective extraction is considered here as follows:

$$I_{\mathrm{cap},\alpha\beta} = sC_f \cdot V_{C,\alpha\beta} \approx sC_f \cdot V_{\mathrm{PCC},\alpha\beta} \tag{12}$$

where it can be seen that the filter capacitor current $I_{\mathrm{cap},\alpha\beta}$ is estimated by the components at a few characteristic frequencies. h is the harmonic order.

Considering that the capacitor current at a specific frequency is 90° leading of the corresponding voltage across the capacitor, a modified bandpass filter $G_{\mathrm{det},h}(s)$ with 90° leading phase shift is used to estimate PCC voltage at each characteristic frequency as follows:

$$G_{\mathrm{det},h}(s) = \frac{-2\omega_{cut}(h\omega_o)}{s^2 + 2\omega_{cut}s + (h\omega_o)^2} \tag{13}$$

where ω_{cut} is bandpass frequency of the extractor, h is the harmonic order, ω_0 is the fundamental angular frequency determined by the PLL. As a result, the center frequency of the extractor in (13) can be adaptive to the small variations of the main grid frequency to achieve an accurate extraction.

Afterward, the capacitor voltage is estimated by multiplying the magnitude of capacitor admittance with the estimated PCC voltage component with leading 90° phase shift

$$\begin{aligned} I_{\mathrm{cap},\alpha\beta} &= \sum_h I_{\mathrm{cap},\alpha\beta,h} \\ &= \sum_h (h\omega_o c_f) \cdot [G_{\mathrm{det},h}(s) \cdot V_{\mathrm{PCC},\alpha\beta}] \\ &= \sum_h \frac{-2\omega_{\mathrm{cut}}(h\omega_o)^2 c_f}{s^2 + 2\omega_{\mathrm{cut}}s + (h\omega_o)^2} \cdot V_{\mathrm{PCC},\alpha\beta}. \end{aligned} \tag{14}$$

The response of the estimator (14) is shown in Fig. 6, where it can be seen this method can accurately estimate the current of the filter capacitor at the selected characteristic frequencies. In addition, the high-frequency ripple current of the capacitor is automatically filtered out by the estimator. Compared to the simple feed-forward term in (11) or the direct derivative operator-based estimation in [41], the proposed grid voltage feed-forward term in (14) can properly emulate the impact of grid harmonic disturbance at selected harmonic frequencies, but without amplifying the harmonics with frequencies close to the resonance frequency of *LCL* filter.

When the capacitor current estimation is obtained in the continuous time domain, the corresponding capacitor current can be expressed in the z-domain using bilinear transformation as

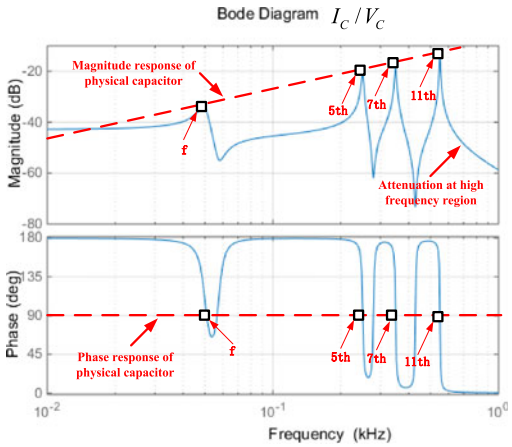

Fig. 6. Frequency domain response of the estimator in (14).

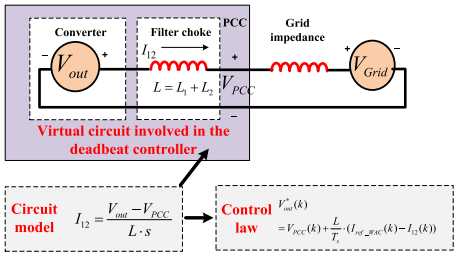

Fig. 7. Implementation of deadbeat controller based on the virtual filter plant.

follows:

$$I_{\mathrm{cap},\alpha\beta}(k) = \sum_h \left. \frac{-2\omega_{\mathrm{cut}}(h\omega_o)^2 c_f}{s^2 + 2\omega_{\mathrm{cut}} s + (h\omega_o)^2} \right|_{s=\frac{2(z-1)}{T_s(z+1)}} \cdot V_{\mathrm{PCC},\alpha\beta}(k) \tag{15}$$

where T_s is the sampling frequency of the system.

B. Principle of the Proposed Controller

The traditional one-step deadbeat current controller can be sensitive to the sampling and processing delay of the system [29], [34], [47]. As a result, many delay compensation methods, including the oversampling method in [25], unsymmetrical sampling and modulation method in [40], and the delay compensated PWM method in [34], were proposed to minimize the impact of processing and sampling delay in a digitally controlled system. When the delays are compensated, the current and voltage signals sampling can be assumed at the beginning of a switching cycle and the deadbeat controller aims to realize zero current tracking errors at the end of the switching cycle [19], [30]–[33]. For a per-phase virtual output filter circuit as shown in Fig. 2(b), the voltage difference $V_{\mathrm{out}} - V_{\mathrm{PCC}}$ can be dynamically regulated to control the weighted average current I_{12} on the choke $L_1 + L_2$. The detailed control law is derived by the process as shown in Fig. 7. Note that the PCC voltage is measured and the voltage drop on the choke $(V_{\mathrm{out}} - V_{\mathrm{PCC}})$ is directly controlled to regulated the weighted average current I_{12}. Thus, the grid impedance only has minor impact of the tracking of weighted average current I_{12}.

If the reference of the line current is given as $I_{\mathrm{ref},\alpha\beta}(k)$ and the difference between the weighted average current and the line current is estimated as $I_{\mathrm{com},\alpha\beta}(k) = \Upsilon I_{\mathrm{cap}}(k)$ according to (8), the reference of weighted average current in Fig. 7 can be derived to ensure an accurate line current regulation as follows:

$$I_{\mathrm{ref\_WAC},\alpha\beta}(k) = I_{\mathrm{ref},\alpha\beta}(k) + I_{\mathrm{comp},\alpha\beta}(k) \tag{16}$$

With this modified reference, the deadbeat controller in the discretized time domain can be given as follows:

$$\begin{aligned} &V^*_{\mathrm{out},\alpha\beta}(k) \\ &= V_{\mathrm{PCC\_ave},\alpha\beta}(k) + \frac{L_1 + L_2}{T_s} \cdot (I_{\mathrm{ref\_WAC},\alpha\beta}(k) - I_{12,\alpha\beta}(k)) \\ &= 1.5V_{\mathrm{PCC},\alpha\beta}(k) - 0.5V_{\mathrm{PCC},\alpha\beta}(k-1) \\ &\quad + \frac{L_1 + L_2}{T_s} \cdot (I_{\mathrm{ref},\alpha\beta}(k) + I_{\mathrm{comp},\alpha\beta}(k) - I_{12,\alpha\beta}(k)) \end{aligned} \tag{17}$$

where $V^*_{\mathrm{out},\alpha\beta}(k)$ is the reference inverter output voltage at the kth switching period, $V_{\mathrm{PCC\_AVE},\alpha\beta}(k)$ is the predicted average PCC voltage at the kth switching period as $1.5V_{\mathrm{PCC},\alpha\beta}(k) - 0.5V_{\mathrm{PCC},\alpha\beta}(k-1)$, $V_{\mathrm{PCC},\alpha\beta}(k)$ and $V_{\mathrm{PCC},\alpha\beta}(k-1)$ are the measured PCC voltage at the beginning of the kth and the $k-1$ th switching period, respectively, $I_{\mathrm{ref},\alpha\beta}(k)$ is the line current reference, $I_{12,\alpha\beta}(k)$ is the weighted average current, and T_s is the switching period.

With this modified deadbeat control in (17), the harmonic of the *LCL* filter can be effectively mitigated, and at the same time, the system has an accurate control of line current at both the steady and the transient states. The mitigation of line current harmonics can be understood in the following way. First, as the weighted average current controller can regulate the weighted average current $I_{12,\alpha\beta}$ on a first-order filter plant with no resonance, the response of $I_{12,\alpha\beta}$ can be ripple free if the corresponding reference current $I_{\mathrm{ref\_WAC},\alpha\beta}$ in (17) is also sinusoidal. However, the current difference $I_{2,\alpha\beta} - I_{12,\alpha\beta} = \Upsilon\, I_{c,\alpha\beta}$ is not addressed by the conventional weighted average control without compensation. Therefore, if $\Upsilon I_{c,\alpha\beta}$ has some harmonic components, the line current $I_{2,\alpha\beta}$ can still be highly distorted. This is particularly serious for *LCL* filters with large shunt capacitor connecting to distorted grid voltage. To address this problem, the compensation term is added to the reference current as $I_{\mathrm{ref\_wac},\alpha\beta} = I_{\mathrm{ref},\alpha\beta} + I_{\mathrm{com},\alpha\beta}$. In this case, the line current $I_{2,\alpha\beta}$ waveform is improved at the expense of some harmonic distortions in the weighted average current $I_{12,\alpha\beta}$.

It is important to note that previous compensation methods that are highly coupled with the current regulator and circuitry parameters and they are usually added to the inner loop reference or the output voltage reference. In this proposed method, compensation term is directly added to the single-loop current reference, resulting in very well decoupled with the current regulators. Therefore, the compensator and the current regulator can be designed independently.

The complete control diagram with three control blocks is shown in Fig. 8. First, the three-phase PCC voltage is measured and this signal is transformed into the quantities in the

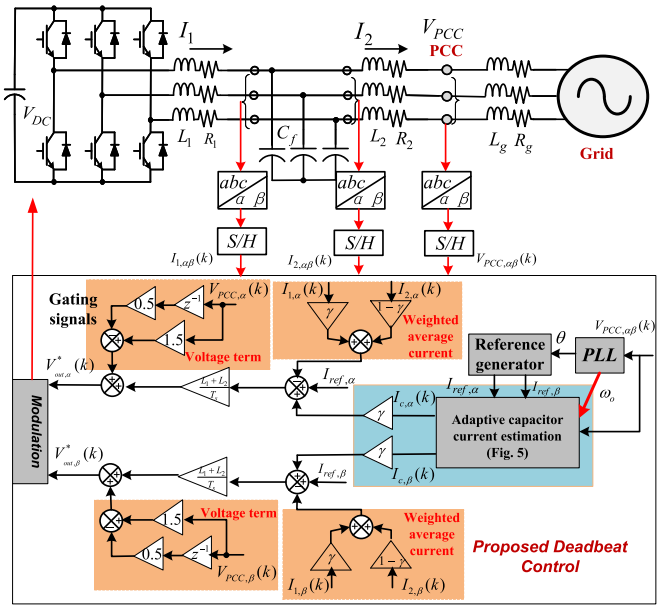

Fig. 8. Diagram of the proposed control deadbeat scheme with weighted average current feedback and line current tracking error compensation.

stationary two-axis reference frame. Afterwards, the average voltage in each switching cycle is estimated. Second, a compensator using PCC voltage feed-forward control is added to the current reference. Third, the weighted average current is calculated and it is regulated by a one-step deadbeat current controller based on the virtual series choke plant in Fig. 7.

Finally, it is necessary to note that the controller in Fig. 8 ensures an accurate control of line current. But when the harmonic-free line current flows to a highly distorted grid, the instantaneous power from the dc link to the PCC has significant ripples. In this case, the dc-link voltage ripple may be amplified [42], [43]. However, as this paper focuses on the compensation of line current harmonics and the switching frequency is much higher than the frequency of dominate dc-link voltage ripples, a further discussion on the dc-link voltage ripple is out of the scope of this paper.

C. Analysis of the Proposed Method

The stability of a converter using the proposed deadbeat controller in (17) has been verified by investigating the root loci in the zero-pole map. Selective analysis results are provided here.

First, the converter circuit parameters are chosen to be the same as these in the real-time simulation, as shown in Table I. When the weighting factor Υ in the proposed current controller changes from 0.8 to 0.2, the root loci of the system are shown in Fig. 9. It can be noticed that there are three moving poles, among which the pole P1 is located in the inner part of the unit cycle and poles P2 and P3 are located in the boundary of the unit cycle. As a result, the performance of the system is more sensitive to the changes of P2 and P3. When the weighting factor is lower than 0.35, P2 and P3 are pushed to the outside of unit cycle, leading to an instable operation of the system.

TABLE I
PARAMETERS OF THE SIMULATED AND EXPERIMENTAL SYSTEM

Circuit Parameter	Value
Rated grid voltage	Three-phase 400 V/50 Hz
DC-link capacitor	$C_{\mathrm{DC}} = 2000\,\mu\mathrm{F}$
LCL filter	$L_1 = 3\,\mathrm{mH} \cdot R_1 = 8\,\mathrm{m\Omega}; C_f = 60\,\mu\mathrm{F}; L_2 = 1.5\,\mathrm{mH}, R_1 = 6\,\mathrm{m\Omega}$
Reference DC-link voltage	600 V
Dead time	$2.5\,\mu\mathrm{s}$
Control parameter	**Value**
Switching frequency	10 kHz
Weighting factor	$\beta = 2/3$
Bandpass angular frequency	$\omega_{\mathrm{cut}} = 0.38$ Hz
Deadbeat controller parameter	$L_1 = 3\,\mathrm{mH}, L_2 = 1.5\,\mathrm{mH}\ t_s = 100\,\mu\mathrm{s}$

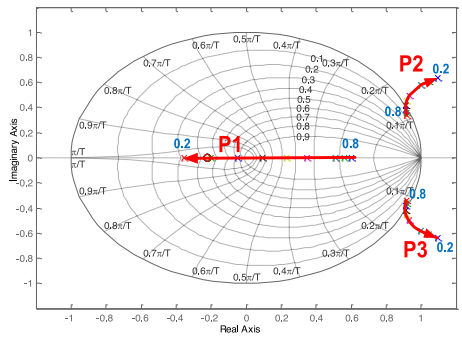

Fig. 9. Root loci of the system when the weighting factor Υ in the proposed deadbeat controller changes from 0.8 to 0.2.

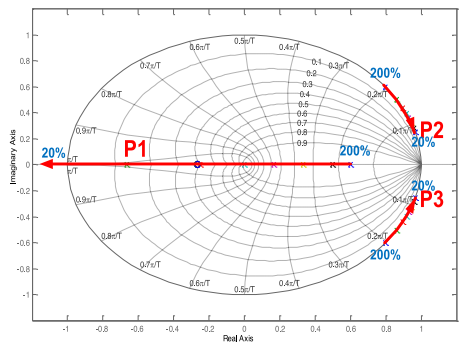

Fig. 10. Root loci of the system when the physical inductances L_1 and L_2 of the *LCL* filter change from 200% to 20% of the nominal value.

Since parameters mismatch often exists in the output *LCL* filter, the stability of the system is also investigated considering the variations of inductance. In this test, fixed parameters ($L_1 = 3\,\mathrm{mH}$, $L_2 = 1.5\,\mathrm{mH}$) are used in the proposed controller in (17), but the physical filter inductance L_1 and L_2 in the output *LCL* filter changes from 200% to 20% of the nominal value. The root loci of the system are shown in Fig. 10. In contrast to Fig. 9 where P2 and P3 can lead to instability of the system, the root loci in Fig. 10 demonstrate that P2 and P3 are stick to the boundary of the unit cycle, but the pole P1 can be pushed to the outside of the unity cycle when the filter inductance is lower than 50% of the nominal value. As a consequence, serious

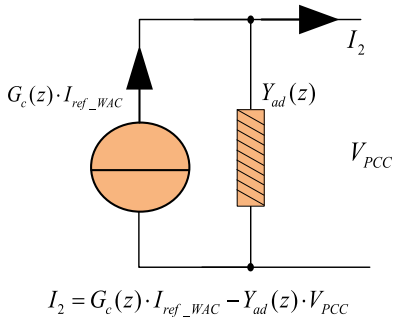

Fig. 11. Closed-loop equivalent circuit of a converter controlled by the proposed method.

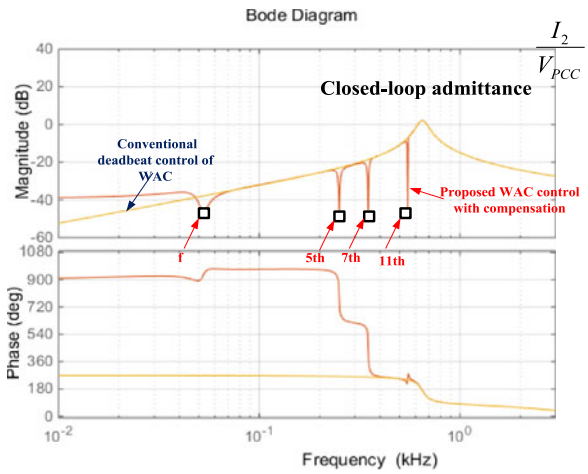

Fig. 12. Frequency domain response of the shunt admittance.

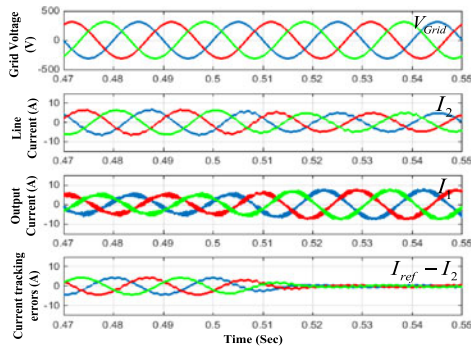

Fig. 13. Performance of the system using the proposed deadbeat control method (compensation term is activated in 0.5 s). (From top to bottom: (a) grid voltage $V_{\rm grid}$; (b) line current I_2; (c) output current I_1; (d) current tracking errors ($I_{\rm ref} - I_2$).)

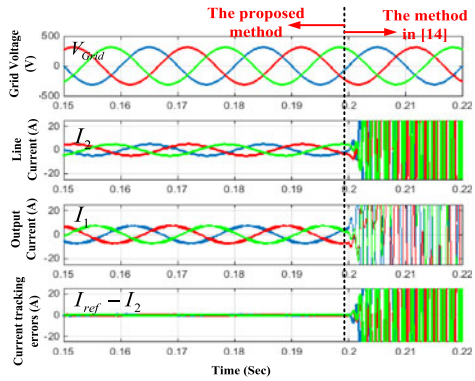

Fig. 14. Performance of the system using the proposed deadbeat control method and the method in [14]. (From top to bottom: (a) grid voltage $V_{\rm grid}$; (b) line current I_2; (c) output current I_1; (d) current tracking errors ($I_{\rm ref} - I_2$)).

inductance attenuations shall be avoided for grid-tied converters using the proposed deadbeat control method.

The performance of line current against grid voltage disturbance is briefly examined here. It has been reported that the closed-loop response of line current can be depicted using a Norton equivalent circuit [6], [50], as shown in Fig. 11. The sensitivity of the line current to PCC voltage disturbance can be examined by the frequency domain response of the shunt admittance $Y_{AD}(z)$ in Fig. 12. From Fig. 12, it can be clearly seen that the shunt admittance at the selected fundamental and low-order harmonic frequencies are attenuated using the proposed feed-forward compensation method, resulting in an improved capability to reject the impact of grid voltage disturbance.

IV. Verification Results

To verify the effectiveness of the proposed control method, comprehensive simulated and experimental results are obtained in this section.

A. Simulated Results

Simulations have been conducted in the MATLAB/Simulink environment. The control and circuitry parameters can be found in Table I. In these simulations, a relatively large shunt capacitor at 60 μF is selected for the *LCL* filter, in order to verify the performance of the proposed method in adverse situations.

First, the weighted average current controller without the compensation term is adopted and the reference current magnitude is set to 5 A. The performance of the system is shown in Fig. 13, where the second and the third channels are the line current and the output current, respectively. It can be seen that the system is stable with sinusoidal line current. Nevertheless, the difference between the reference current and the line current as shown at the bottom of this figure is around 4.5 A, which is obviously not acceptable for low-power converters. When the compensation term $I_{\mathrm{comp},\alpha\beta}(k)$ using PCC voltage feed-forward is adopted to reduce the line current tracking errors at 0.5 s, the waveform of line current is still sinusoidal but the line current tracking error reduces to less than 0.65 A in this test.

As mentioned earlier, the stability of the conventional current controlled system can hardly be maintained when designing the control parameters without properly considering the effects of large shunt capacitor. This conclusion is examined as demonstrated in Fig. 14. In the beginning of the simulation, the stable operation of the system is achieved by using the proposed weighted average current control method with

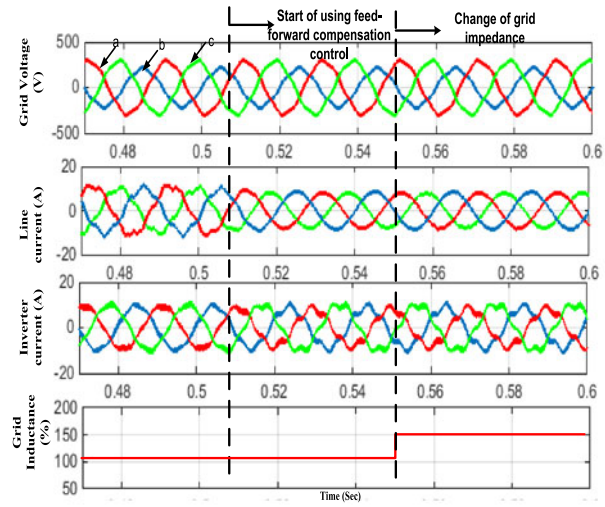

(a)

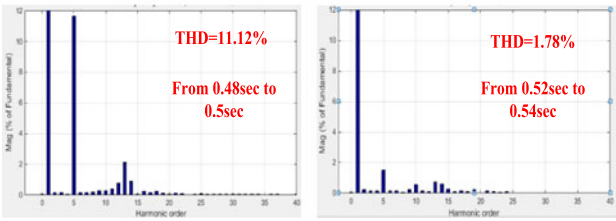

(b)

Fig. 15. Performance of the system using the proposed method, operating in a distorted grid with grid impedance variation. (a) From top to bottom: (1) Grid voltage V_{grid}; (2) line current I_2; (3) output current I_1; (4) main grid inductance L_g. (b) Harmonic spectrum of line current before and after the use of the feed-forward compensation.

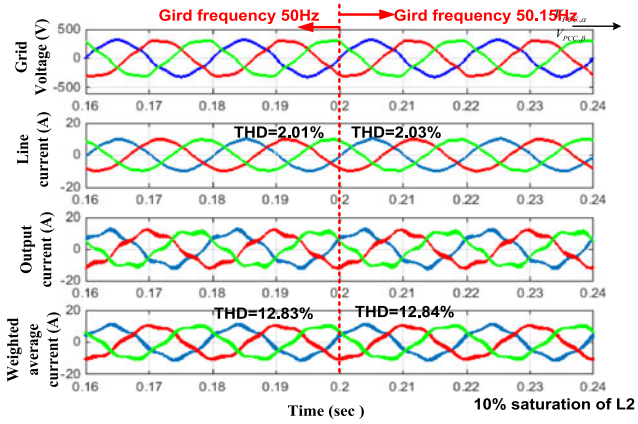

Fig. 16. Performance of the system using the proposed deadbeat control method with feed-forward control. Grid frequency changes from 50 to 50.15 Hz at 0.2 s. (From top to bottom: (a) Grid voltage V_{Grid}; (b) line current I_2; (c) output current I_1; (d) weighted average current I_{12}).

feed-forward compensation. At the time 0.2 s, the well-understood PR current control method with lead–leg compensator in [14] is applied to the system and the PR control parameters are determined according to the design guideline. It can be clearly seen that the system immediately becomes unstable when the conventional controller is applied to the system.

The performance of the system under adverse grid voltage situation with rich harmonics is also tested, as shown in Fig. 15. In this simulation, 5% 5th harmonics and 0.8 11th harmonics are added to the main grid voltage. In the beginning of the test, the deadbeat weighted average current control without using the feed-forward compensation is applied to the system. As there is insufficient rejection against grid voltage harmonics disturbances, it can be noticed that the line current is highly distorted and the total harmonic distortion (THD) of the line current is 11.12%.

When the proposed feed-forward control using the estimator in Fig. 5(b) is activated at 0.5 s, it can be seen that the line current harmonics are mitigated and the corresponding THD is only 1.78%. It is important to emphasis that when a three-phase balanced current is injected into a highly distorted grid or imbalanced grid, the instantaneous output power has some oscillation [51]. They are some methods to dynamically regulate the oscillations in both real and reactive power. However, a deeper analysis is out of the scope of this paper. At 0.55 s, the grid impedance of the system increases to 150% of the nominal value, the waveforms in Fig. 15 also demonstrates that the system line current control is not affected. From the above tests, it can be concluded that the proposed method with feed-forward control is insensitive to the variation of grid impedance or the harmonic disturbances from the main grid. The detailed spectrum for the line current in Fig. 15(a) is shown in Fig. 15(b) for comparison.

To test the performance of the system when the main grid voltage frequency has some variations, more simulations are conducted and the results are shown in Figs. 16–18, where the main grid has 6.5% harmonic distortions. First, an enhanced performance using the proposed method with adaptive frequency extractor-based feed-forward control is illustrated in Fig. 16, where it can be clearly seen that line current is sinusoidal before and after the change of grid voltage frequency. At the same time, the inverter output current is distorted as the harmonic current from the shunt capacitor are inherently compensated by the inverter output current.

To have a better understanding of the principle of line current harmonic compensation, the performance of the system using the deadbeat control method but without the feed-forward control is given in Fig. 17. As the weighted average current reference is a sine wave in this case, the weighted average current as shown at the bottom of Fig. 17 has very good quality with only 5.01% THD. Note that the dominate distortion in the weighted average current comes from the switching ripple of I_1 Nevertheless, the almost ripple-free weighted average current cannot guarantee an enhanced quality of line current that injects into the main grid. The THD of the line current in Fig. 17 is 12.91%.

According to the previous analysis, the feed-forward control is not always effective if other current regulators are used. To verify this conclusion, the deadbeat controller is replaced by

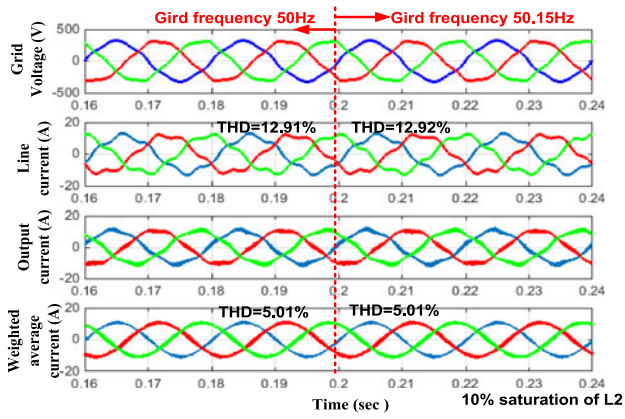

Fig. 17. Performance of the system using the proposed deadbeat control method but without feed-forward control. Grid frequency changes from 50Hz to 50.15Hz at 0.2sec. (From top to bottom: (a) Grid voltage V_{Grid}; (b) line current I_2; (c) output current I_1; (d) weighted average current I_{12}).

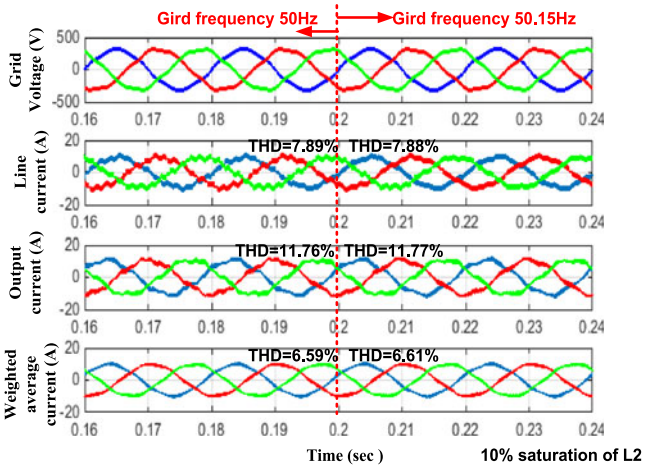

Fig. 18. Performance of the system using the PI control for weighted average current regulation, with feed-forward control. Grid frequency changes from 50 to 50.15 Hz at 0.2 s. (From top to bottom: (a) Grid voltage V_{Grid}; (b) line current I_2; (c) output current I_1; (d) weighted average current I_{12}).

the PI controller in the rotating reference frame in [23] and the corresponding performance with feed-forward control is shown in Fig. 18. As indicated in the second channel of this figure, the line current harmonic in this case cannot be properly mitigated when using PI regulator with reduced control bandwidth.

B. Experimental Results

Experimental results have been obtained from a laboratory three-phase converter prototype. The detailed system parameters are also listed in Table I. The dc-link voltage is powered up by an isolated dc-power supply.

In the first test, the proposed weighted average current regulator without using PCC voltage feed-forward control is applied to the system. The magnitude of the reference current is set to 10 A. The steady-state performance of the converter line current is illustrated in the middle of Fig. 19. The bottom waveform

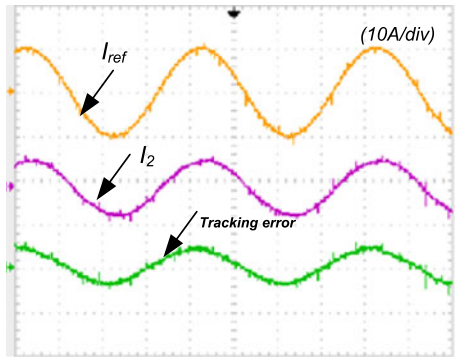

Fig. 19. Performance of the system using the proposed deadbeat control method but without using the compensation term. (From top to bottom: (a) reference current I_{ref}; (b) line current I_2; (c) current tracking errors ($I_{\mathrm{ref}} - I_2$)).

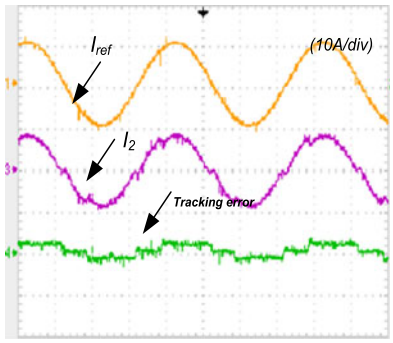

Fig. 20. Performance of the system using the proposed deadbeat control method. The compensation term is determined by differential operation. (From top to bottom: (a) reference current I_{ref}; (b) line current I_2; (c) current tracking errors ($I_{\mathrm{ref}} - I_2$)).

shown at the bottom of Fig. 19 depicts that there are significant steady-state current tracking errors in the line current.

When the filter capacitor current is estimated by using a direct derivative operation, the performance of the system is shown in Fig. 20. Comparing to the performance in Fig. 19, it can be noticed that the adoption of derivative operation-based filter capacitor current estimation can improve the line current tracking accuracy. Nevertheless, the tracking errors as shown at the bottom of Fig. 20 are still noticeable and there are some harmonics in the tracking errors.

When the proposed deadbeat control of weighted average current with the feed-forward term using the estimator in Fig. 5(b) is applied to the system, the enhanced performance is shown in Fig. 21. In this case, the waveform of converter line current in the middle of the figure is fairly close to the reference current as shown in the top. Accordingly, the current tracking error as illustrated in the bottom is around zero. Due to the removal of differential operation in the estimation of capacitor current, the line current in this case is highly smooth with only 2.58% THD.

The performance of the proposed controller under the situation of significant filter parameter variations is also compared with some well-understood controllers. In this test, the converter side choke L_1 and the line side choke L_2 are 2.0 and 1.2 mH, respectively. To fully demonstrate the impact of choke inductance

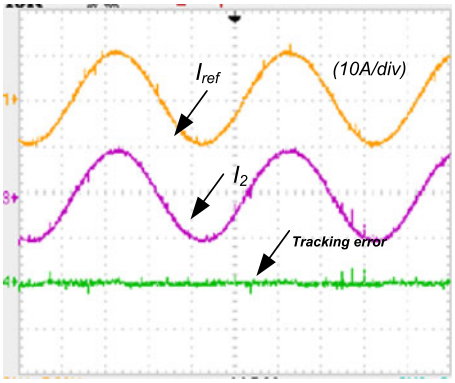

Fig. 21. Performance of the system using the proposed deadbeat control method with the proposed compensation term. (From top to bottom: (a) reference current $I_{\rm ref}$; (b) line current I_2; (c) current tracking errors ($I_{\rm ref} - I_2$)).

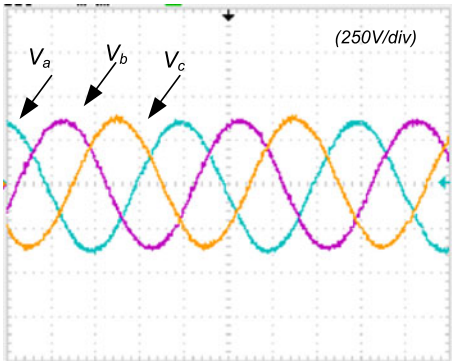

Fig. 22. Steady-state three-phase grid voltage.

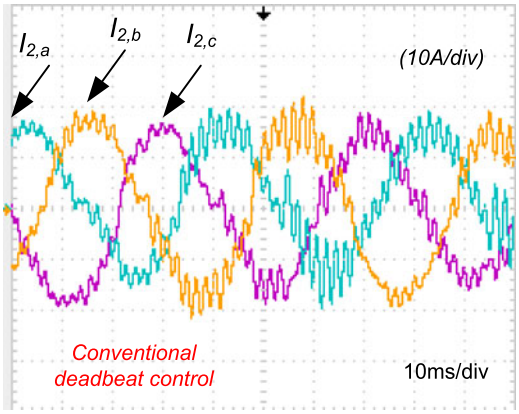

Fig. 23. Steady-state performance of the method in [28].

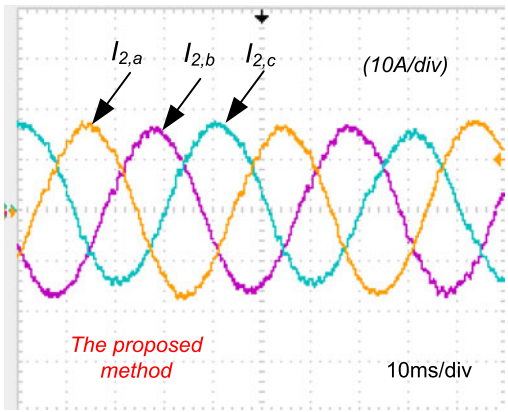

Fig. 24. Steady-state performance of the system using the proposed method with feed-forward compensation.

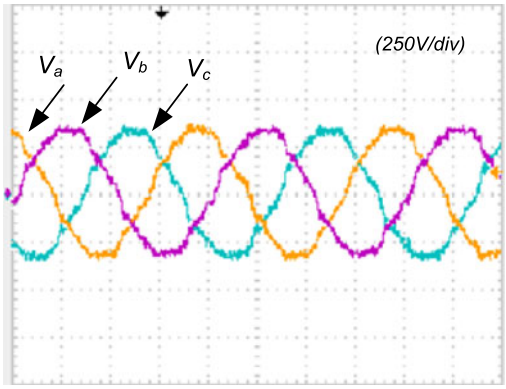

Fig. 25. Highly distorted three-phase grid voltage.

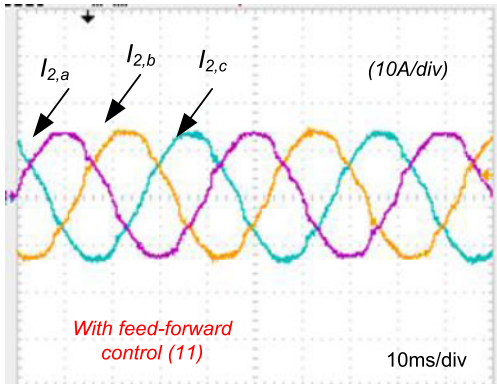

Fig. 26. An enhanced performance using the proposed deadbeat control with PCC voltage feed-forward compensation.

mismatch to line current resonance, a ripple-free three-phase grid voltage is used here, as shown in Fig. 22.

First, when the deadbeat controller with pole-zero cancellation-based active damping in [28] is applied to the system, the performance is captured in Fig. 23. It can be seen that with significant parameters variations, conventional pole-zero cancellation-based active damping can hardly suppress the resonance current. When the deadbeat control of weighted average current with a proposed feed-forward compensator is applied to system, the resonance in the line current is still effectively mitigated, as shown in Fig. 24.

When the main grid has significant distortions with 6.0% 5th, 1.0% 7th, 1.0% 11th and 0.8% 13th harmonic voltages as shown in Fig. 25,the performance of the system is also verified. In this test, an enhanced performance using the proposed deadbeat control with PCC voltage feed-forward in (16) and (17) is shown in

Fig. 26, where it can be seen that the line current low-frequency distortions are mitigated and the THD is only 5.99%.

V. Conclusion

An enhanced current controller is proposed in this paper. The research work of this paper is summarized here:

1) in order to realize rapid control of converter current, the deadbeat control is applied to regulate the weighted average current based on a virtual filter plant;
2) the feed-forward compensator is developed to mitigate the steady-state fundamental current tracking errors caused by conventional weighted average current control;
3) the frequency-selective capacitor leg current estimation is proposed and the corresponding compensation term can be used to increase the robustness of the converter against grid harmonic distortions. The design and implementation of this compensator are highly decoupled from the closed-loop deadbeat current regulator. Thus, both the current regulator and the compensator can be independently designed.

References

[1] F. Blaabjerg, Z. Chen, and S. B. Kjaer, "Power electronics as efficient interface in dispersed power generation systems," *IEEE Trans. Power Electron.*, vol. 19, no. 5, pp. 1184–1194, May 2004.

[2] J. Rocabert, A. Luna, F. Blaabjerg, and P. Rodriguez, "Control of power converters in AC microgrids," *IEEE Trans. Power Electron.*, vol. 27, no. 11, pp. 4734–4749, Nov. 2012.

[3] Y. W. Li, D. M. Vilathgamuwa, and P. C. Loh, "Design, analysis and real-time testing of a controller for multibus microgrid system," *IEEE Trans. Power Electron.*, vol. 19, no. 5, pp. 1195–1204, Sep. 2004.

[4] J. M. Guerrero, L. G. Vicuna, J. Matas, M. Castilla, and J. Miret, "A wireless controller to enhance dynamic performance of parallel inverters in distributed generation systems," *IEEE Trans. Power Electron.*, vol. 19, no. 4, pp. 1205–1213, Sep. 2004.

[5] J. He and Y. W. Li, "Hybrid voltage and current control approach for DG-grid interfacing converters with LCL filters," *IEEE Trans. Ind. Electron*, vol. 60, pp. 1797–1809, May 2013.

[6] C-L. Chen, Y. Wang, J-S. Lai, Y-S. Lee, and D. Martin, "Design of parallel inverters for smooth mode transfer microgrid application," *IEEE Trans. Power Electron.*, vol. 25, no. 1, pp. 6–15, Jan. 2010.

[7] P. C. Loh and D. G. Holmes, "Analysis of multiloop control strategies for LC/CL/LCL-filtered voltage-source and current source inverters," *IEEE Trans Ind. Appl.*, vol. 41, no. 2, pp. 644–654, Mar./Apr. 2005.

[8] J. He and Y. W. Li, "Generalized closed-loop control schemes with embedded virtual impedances for voltage source converters with LC or LCL filter," *IEEE Trans. Power Electron.*, vol. 27, no. 4, pp. 1850–1861, Apr. 2012.

[9] J. S. Lim, C. Park, J. Han, and Y. Lee II., "Robust tracking control of a three-phase DC-AC inverter for UPS applications," *IEEE Trans. Ind. Electron.*, vol. 61, no. 8, pp. 4142–4151, Aug. 2014.

[10] G. Lo-Calzo, A. Lidozzi, L. Solero, and F. Crescimbini, "LC filter design for on-grid and off-grid distributed generating units," *IEEE Trans. Ind. Appl.*, vol. 51, no. 2, pp. 1639–1650, Mar./Apr. 2015.

[11] T. G. Habetler, R. Naik, and T. A. Nondahl, "Design and implementation of an inverter output LC filter used for dv/dt reduction," *IEEE Trans. Power Electron.*, vol. 17, no. 3, pp. 327–331, May 2002.

[12] M. Liserre, F. Blaabjerg, and S. Hansen, "Design and control of an LCL-filter-based three-phase active rectifier," *IEEE Trans. Ind. Appl.*, vol. 41, no. 5, pp. 1281–1291, Sep./Oct. 2005.

[13] A. A. Rockhill, M. Liserre, R. Teodorescu, and P. Rodriguez, "Grid-filter design for a multimegawatt medium-voltage voltage source inverter," *IEEE Trans. Ind. Electron.*, vol. 58, no. 4, pp. 1205–1217, Apr. 2011.

[14] M. Liserre, R. Teodorescu, and F. Blaabjerg, "Stability of photovoltaic and wind turbine grid-connected inverters for a large set of grid impedance values," *IEEE Trans. Ind. Appl.*, vol. 42, no. 5, pp. 1146–1154, Sep./Oct. 2006.

[15] A. Timbus, M. Liserre, R. Teodorescu, P. Rodriguez, and F. Blaabjerg, "Evaluation of current controllers for distributed power generation systems," *IEEE Trans. Power Electron.*, vol. 24, no. 3, pp. 654–664, Mar. 2009.

[16] E. Twining and D. G. Holmes, "Grid connected regulation of a three-phase voltage source inverter with an LCL input filter," *IEEE Trans. Power Electron.*, vol. 18, no. 3, pp. 888–895, May 2003.

[17] M. H. Bierhoff and F. W. Fuchs, "Active damping for three-phase PWM rectifiers with high-order line-side filters," *IEEE Trans. Ind. Electron.*, vol. 56, no. 2, pp. 371–379, Feb. 2010.

[18] S. Eren, M. Pahlevaninezhad, A. Bakhshai, and P. K. Jain, "Composite nonlinear feedback control and stability analysis of a grid connected voltage source inverter with LCL filter," *IEEE Trans. Ind. Electron.*, vol. 60, no. 11, pp. 5059–5074, Nov. 2013.

[19] Y. A.-R. I. Mohamed and E. F. EI-Saadany, "An improved deadbeat current control scheme with a novel adaptive self-tuning load model for a three-phase PWM voltage-source inverter," *IEEE Trans. Ind. Electron.*, vol. 54, no. 2, pp. 747–759, Apr. 2007.

[20] J. Kukkola and M. Hinkkanen, "Observer-based state-space current control for a three-phase grid-connected converter equipped with an LCL filter," *IEEE Trans. Ind. Appl.*, vol. 50, no. 4, pp. 2700–2709, Jul./Aug. 2014.

[21] G. Shen, X. Zhu, J. Zhang, and D. Xu, "A new feedback method for PR current control of LCL-filter-based grid-connected inverters," *IEEE Trans. Ind. Electron.*, vol. 57, no. 6, pp. 2033–2041, Jun. 2010.

[22] G. Shen, D. Xu, L. Cao, and X. Zhu, "An improved control strategy for grid-connected voltage source inverters with an LCL filter," *IEEE Trans. Power Electron.*, vol. 23, no. 4, pp. 1899–1906, Jan. 2008.

[23] N. He, D. Xu, Y. Zhu, J. Zhang, G. Shen, Y. Zhang, J. Ma, and C. Liu, "Weighted average current control in a three-phase grid inverter with an LCL filter," *IEEE Trans. Power Electron.*, vol. 28, no. 6, pp. 2785–2797, Jun. 2013.

[24] J. He, Y. W. Li, D. Bosnjak, and B. Harris, "Investigation and active damping of multiple resonances in a parallel-inverter-based microgrid," *IEEE Trans. Power Electron.*, vol. 28, no. 1, pp. 234–246, Jan. 2013.

[25] Q. Zeng and L. Chang, "An advanced SVPWM-based predictive current controller for three-phase inverters in distributed generation systems," *IEEE Trans. Ind. Electron.*, vol. 55, no. 3, pp. 1235–1246, Mar. 2008.

[26] T.-L. Lee, J.-C. Li, and P.-T. Cheng, "Discrete frequency tuning active filter for power system harmonics," *IEEE Trans. Power Electron.*, vol. 24, no. 5, pp. 1209–1217, May 2009.

[27] K. H. Ahmed, A. M. Massoud, S. J. Finney, and B. W. Williams, "A modified stationary reference frame-based predictive current control with zero steady-state error for LCL coupled inverter-based distributed generation systems," *IEEE Trans. Ind. Electron*., vol. 58, no. 4, pp. 1359–1370, Apr. 2011.

[28] E. Wu and P. W. Lehn, "Digital current control of a voltage source converter with active damping of LCL resonance," *IEEE Trans. Power Electron.*, vol. 21, no. 5, pp. 1364–1373, Sep. 2006.

[29] H. Abu-Rub, J. Guzinski, Z. Krzeminski, and H. Toliyat, "Predictive current control of voltage-source inverters," *IEEE Trans. Ind. Electron*, vol. 51, no. 3, pp. 585–593, Jun. 2004.

[30] D. Martion and E. Santi, "Auto tuning of digital deadbeat current controller for grid tied inverters using wide bandwidth impedance identification," in *Proc. IEEE 27th Annu. Appl. Power Electron. Conf.*, Feb. 5–9, 2012, pp. 277–284.

[31] S. Saggini, W. Stefanutti, E. Tedeschi, and P. Mattavelli, "Digital deadbeat control tuning for dc-dc converters using error correlation, " *IEEE Trans. Power Electron.*, vol. 22, no. 4, pp. 1566–1570, Jul. 2007.

[32] Y. Zhang, W. Xie, and Y. Zhang, "Deadbeat direct power control of three-phase pulse-width modulation rectifiers," *IET Power Electron.*, vol. 7, no. 6, pp. 1340–1346, Jul. 2014.

[33] K. H. Ahemd, A. M. Massoud, S. J. Finney, and B. W. Williams, "A modified stationary reference frame-based predictive current control with zero steady-state error for LCL coupled inverter-based distributed generation systems," *IEEE Trans. Ind. Electron.*, vol. 58, no. 4, pp. 1359–1370, Apr. 2011.

[34] H. Deng, R. Oruganti, and D. Srinivasan, "PWM methods to handle time delay in digital control of a UPS," *IEEE Power Electron Lett.*, vol. 3, no. 1, pp. 1–6, Mar. 2005.

[35] S. G. Parker, B. P. McGrath, and D. G. Holmes, "Regions of active damping control for LCL filters," *IEEE Trans. Ind. Appl.*, vol. 50, no. 1, pp. 424–432, Jan./Feb. 2014.
[36] D. Pan, X. Ruan, C. Bao, W. Li, and X. Wang, "Optimized controller design of LCL-type grid-connected inverter to achieve high robustness against grid-impedance variation," *IEEE Trans. Ind. Electron.*, vol. 62, no. 3, pp. 1537–1547, Mar. 2015.
[37] D. Pan, X. Ruan, C. Bao, W. Li, and X. Wang, "Capacitor-current-feedback active damping with reduced computation delay for improving robustness of LCL-type grid-connected inverter," *IEEE Trans. Power Electron.*, vol. 29, no. 7, pp. 3414–3427, Jul. 2014.
[38] D. Pan, X. Ruan, C. Bao, W. Li, and X. Wang, "Full-feedforward schemes of grid voltage for a three-phase LCL-type grid-connected inverter," *IEEE Trans. Ind. Electron.*, vol. 60, no. 6, pp. 2237–2250, Jun. 2013.
[39] R. Pena-Alzola, M. Liserre, F. Blaabjerg, R. Sebastian, J. Dennehl, and F. W. Fuchs, "Systematic design of the lead–lag network method for active damping in LCL-filter based three-phase converters," *IEEE Trans. Ind. Informat.*, vol. 10, no. 1, pp. 43–52, May 2013.
[40] H. M. Kojabadi, B. Yu, I. A. Gadoura, L. Chang, and M. Ghribi, "A novel DSP-based current controlled PWM strategy for single phase grid connected inverters," *IEEE Trans. Power Electron.*, vol. 21, no. 4, pp. 327–331, Jul. 2006.
[41] M. A. Herran, J. R. Fischer, S. A. Gonzalez, M. G. Judewicz, I. Carugati, and D. O. Carrica, "Repetitive control with adaptive sampling frequency for wind power generation systems," *IEEE J. Emerg. Sel. Topics Power Electron.*, vol. 2, no. 1, pp. 58–69, Mar. 2014.
[42] Z. Li, Y. Li, P. Wang, H. Zhu, C. Liu, and W. Xu, "Control of three-phase boost-type PWM rectifier in stationary frame under unbalanced input voltage," *IEEE Trans. Power Electron.*, vol. 25, no. 10, pp. 2521–2530, Oct. 2010.
[43] Y. Zhang and C. Qu, "Model predictive direct power control of PWM rectifiers under unbalanced network conditions," *IEEE Trans. Ind. Electron.*, vol. 62, no. 7, pp. 4011–4022, Jul. 2015.
[44] J. Yin, S. Duan, and B. Liu, "Stability analysis of grid-connected inverter with LCL filter adopting a digital single-loop controller with inherent damping characteristic," *IEEE Trans. Ind. Informat.*, vol. 9, no. 2, pp. 1104–1112, May 2013.
[45] J. Dannehl, M. Liserre, and F. Fuchs, "Filter-based active damping of voltage source converters with LCL filter," *IEEE Trans. Ind. Electron.*, vol. 58, no. 8, pp. 3623–3633, Aug. 2011.
[46] C. Busada, S. Gomez Jorge, A. Leon, and J. Solsona, "Current controller based on reduced order generalized integrators for distributed generation systems," *IEEE Trans. Ind. Electron.*, vol. 59, no. 7, pp. 2898–2909, Jul. 2012.
[47] J. Fischer, S. Gonzalez, M. Herran, M. Judewicz, and D. Carrica, "Calculation-delay tolerant predictive current controller for three-phase inverters," *IEEE Trans. Ind. Inf.*, vol. 5, no. 2, pp. 55–65, Feb. 2013.
[48] J. He, Y. W. Li, X. Wang, and F. Blaabjerg, "Active harmonic filtering using current controlled grid-connected DG units with closed-loop power control," *IEEE Trans. Power Electron.*, vol. 29, pp. 642–653, Feb. 2014.
[49] W. Wang, A. Beddard, A. M. Barnes, and O. Marjanovic, "Analysis of active power control for VSC–HVDC" *IEEE Trans. Power Del.*, vol. 29, no. 4, pp. 1978–1988, Dec. 2014.
[50] F. Wang, J. L. Duarte, and M. A. M. Hendrix, "Grid-interfacing converter systems with enhanced voltage quality for microgrid application—Concept and implementation," *IEEE Trans. Power Electron.*, vol. 26, no. 12, pp. 3501–3513, Dec. 2011.
[51] A. Camacho, M. Castilla, J. Miret, R. Guzman, and A. Borrell, "Reactive power control for distributed generation power plants to comply with voltage limits during grid faults," *IEEE Trans. Power Electron.*, vol. 29, no. 11, pp. 6224–6234, Nov. 2014.
[52] R. Teodorescu, F. Blaabjerg, M. Liserre, and A. Dell'Aquila, "A stable three-phase LCL-filter based active rectifier without damping," in *Proc. Conf. Rec. 38th Ind. Appl. Soc. Annu. Meeting*, 2003, pp. 1552–1557.
[53] M. Xue, Y. Zhang, Y. Kang, Y. Yi, S. Li, and F. Liu, "Full feedforward of grid voltage for discrete state feedback controlled grid-connected inverter with LCL filter," *IEEE Trans. Power Electron.*, vol. 27, no. 10, pp. 4234–4247, Oct. 2012.
[54] X. Wang, X. Ruan, S. Liu, and C. K. Tse, "Full feedforward of grid voltage for grid-connected inverter with LCL filter to suppress current distortion due to grid voltage harmonics," *IEEE Trans. Power Electron.*, vol. 25, no. 12, pp. 3119–3127, Dec. 2010.
[55] X. Wu, X. Li, X. Yuan, and Y. Geng, "Grid harmonics suppression scheme for LCL-type grid-connected inverters based on output admittance revision," *IEEE Trans. Sustain. Energy*, vol. 6, no. 2, pp. 411–421, Feb. 2015.

Jinwei He received the B.Sc. degree from Southeast University, Nanjing, China, the M.Sc. degree from the Institute of Electrical Engineering, Chinese Academy of Sciences, Beijing, China, and the Ph.D. degree from the University of Alberta, Edmonton, Canada, all in electrical engineering, in 2005, 2008, and 2013, respectively.

In September 2015, he joined Tianjin University, Tianjin, China, where he is currently a Professor. His research interests include power electronics for microgrid and distributed power generation.

Yun Wei Li received the B.Sc. degree in electrical engineering from Tianjin University, Tianjin, China, in 2002, and the Ph.D. degree from Nanyang Technological University, Singapore, in 2006.

In 2005, he was a Visiting Scholar with Aalborg Univ ersity, Denmark. From 2006 to 2007, he was a Postdoctoral Research Fellow with Ryerson University, Canada. In 2007, he worked with Rockwell Automation, Canada, and later joined the Department of Electrical and Computer Engineering, University of Alberta, Canada, in the same year. He is currently a Professor at University of Alberta, Edmonton, Canada. His research interests include distributed generation, microgrid, renewable energy, high-power converters and electric motor drives.

Dr. Li serves as an Associate Editor for the IEEE TRANSACTIONS ON POWER ELECTRONICS and the IEEE TRANSACTIONS ON INDUSTRIAL ELECTRONICS. He also worked as a Guest Editor for the IEEE TRANSACTIONS ON INDUSTRIAL ELECTRONICS Special Session on Distributed Generation and Microgrids. He received the 2013 Richard M. Bass Outstanding Young Power Electronics Engineer Award from the IEEE POWER ELECTRONICS SOCIETY.

Dehong Xu received the Ph.D. degree from the Department of Electrical Engineering, Zhejiang University, China, in 1989.

He became a Full Professor in Zhejiang University in 1996. He was a Visiting Professor with the Department of Electrical Engineering, University of Tokyo, Japan, from May 1995 to June 1996, and Center of Power Electronics System, Virginia Tech, USA, from June to December of 2000 and Power Electronics Lab, ETH, Zurich in 2006, respectively. His research interests include power electronics topology, control, and applications to renewable energy and energy efficiency. He has authored six books and more than 200 IEEE Journal or Conference papers. He holds more than 30 Chinese patents and 3 U.S. patents.

Dr. Xu was at-large Adcom Member of the IEEE Power Electronics Society from 2006 to 2008. He was the General Chair of IEEE International Symposium on Industrial Electronics (ISIE2012, Hangzhou), IEEE International Symposium on Power Electronics for Distributed Generation Systems (PEDG2013, Arkansas), IEEE Power Electronics and Applications (PEAC2014, Shanghai), and International Future Energy Challenge Competition (IFEC2015). He is currently an Associate Editor of the IEEE TRANSACTION ON POWER ELECTRONICS and the IEEE TRANSACTION ON SUSTAINABLE ENERGY. He has been an IEEE PELS Distinguish Lecturer since 2015. Since 2013, he has been the President of China Power Supply Society. He has received four IEEE journal or conference prize paper awards.

Xiaodong Liang was born in Lingyuan, China. She received the B.Eng. and M.Eng. degrees from Shenyang Polytechnic University, Shenyang, China, in 1992 and 1995, respectively, the M.Sc. degree from the University of Saskatchewan, Saskatoon, SK, Canada, in 2004, and the Ph.D. degree from the University of Alberta, Edmonton, AB, Canada, in 2013, all in electrical engineering.

From 1995 to 1999, she served as a Lecturer with Northeastern University, Shenyang, China. In October 2001, she joined Schlumberger, Edmonton, AB, Canada. She was a Principal Power Systems Engineer with this large oil service company before joining Washington State University, Vancouver, WA, USA, in August 2013. From August 2013 to May 2015, she was an Assistant Professor with Washington State University. In July 2015, she joined Memorial University of Newfoundland, St. John's, NL, Canada, where she is currently an Assistant Professor. Her research interests include power system dynamics, power quality, and electric machines.

Dr. Liang is a Registered Professional Engineer in the Provinces of Alberta and Newfoundland and Labrador, Canada.

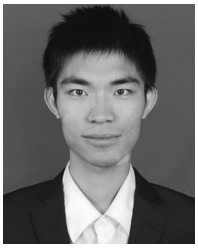

Beihua Liang received the B.Sc. degree from Tianjin University, Tianjin, China, in 2014, where he is currently working toward the Ph.D. degree.

His research interests include power electronics for microgrid and distributed power generation.

Chengshan Wang received the Ph.D. degree in electrical engineering from Tianjin University, Tianjin, China, in 1991.

He is currently a Professor at the School of Electrical Engineering and Automation, Tianjin University. His research interests include distributed generation and microgrids, power distribution system analysis and planning, power system security analysis.